Check for updates

CHEMISTRY
AN ASIAN JOURNAL
www.chemasianj.org

Accepted Article

Title: A Design Strategy for Single-Stranded Helicates using Pyridine-Hydrazone Ligands and PbII ions. Maureen J. Lobo, Stephen C. Moratti, and Lyall R. Hanton*[a]

Authors: Maureen Jean Lobo, Stephen Carl Moratti, and Lyall Robert Hanton

This manuscript has been accepted after peer review and appears as an Accepted Article online prior to editing, proofing, and formal publication of the final Version of Record (VoR). This work is currently citable by using the Digital Object Identifier (DOI) given below. The VoR will be published online in Early View as soon as possible and may be different to this Accepted Article as a result of editing. Readers should obtain the VoR from the journal website shown below when it is published to ensure accuracy of information. The authors are responsible for the content of this Accepted Article.

To be cited as: *Chem. Asian J.* 10.1002/asia.201801784

Link to VoR: http://dx.doi.org/10.1002/asia.201801784

A Journal of

ACES Asian Chemical Editorial Society

A sister journal of **Angewandte Chemie** and **Chemistry – A European Journal**

WILEY-VCH

10.1002/asia.201801784

WILEY-VCH

FULL PAPER

A Design Strategy for Single-Stranded Helicates using Pyridine-Hydrazone Ligands and Pb^{II}

Maureen J. Lobo, Stephen C. Moratti, and Lyall R. Hanton*[a]

Abstract: The reactions of py-hz ligands (**L1-L5**) with $Pb(CF_3SO_3)_2{\cdot}H_2O$ resulted in some rare examples of discrete single-stranded helical Pb^{II} complexes. **L1** and **L2** formed non-helical mononuclear complexes $[Pb\mathbf{L1}(CF_3SO_3)_2]{\cdot}CHCl_3$ and $Pb\mathbf{L2}(CF_3SO_3)_2][Pb\mathbf{L2}CF_3SO_3]CF_3SO_3{\cdot}CH_3CN$, which reflected the high coordination number and effective saturation of Pb^{II} by the ligands. The reaction of **L3** with Pb^{II} resulted in a dinuclear *meso*-helicate $[Pb_2\mathbf{L3}(CF_3SO_3)_2Br]CF_3SO_3{\cdot}CH_3CN$ with a stereochemically-active lone pair on Pb^{II}. **L4** directed single-stranded helicates with Pb^{II}, including $[Pb_2\mathbf{L4}(CF_3SO_3)_3]CF_3SO_3{\cdot}CH_3CN$ and $[Pb_2\mathbf{L4}CF_3SO_3(CH_3OH)_2](CF_3SO_3)_3{\cdot}2CH_3OH{\cdot}2H_2O$. The acryloyl-modified py-hz ligand **L5** formed helical and non-helical complexes with Pb^{II}, including a trinuclear Pb^{II} complex $[Pb_3\mathbf{L5}(CF_3SO_3)_5]CF_3SO_3{\cdot}3CH_3CN{\cdot}Et_2O$. The high denticity of the long-stranded py-hz ligands **L4** and **L5** was essential to the formation of single-stranded helicates with Pb^{II}.

Introduction

As a step towards realising useful motion of molecular machines, the organisation of dynamic molecules into larger assemblies continues to attract interest. *N*-Heterocyclic-hydrazone ligands are a class of molecules that have significant differences in shape between their metal-coordinated and uncoordinated states.[1] α,α-Pyridine-hydrazones (py-hz) are known to adopt a linear shape in solution through minimising unfavourable interactions between the neighbouring nitrogen lone pairs. Upon metal ion binding, however, the py-hz ligands rearrange into helical shapes.[2] The difference in conformation between the uncoordinated and coordinated states of *N*-heterocyclic hydrazone ligands has been associated with a dynamic motional behaviour in solution.[3] However, the metal-induced conformational changes of *N*-heterocyclic hydrazone ligands ligands has so far been limited to the solution state. The incorporation of such molecules into polymer gels could produce movement that is visible on a large scale.

Early metal coordination studies of py-hz ligands focused on derivatives of pyridine-2,6-dicarbaldehyde that formed non-helical mononuclear complexes with Co(II) and Zn(II).[4] More recently, emphasis has been placed on generating dinuclear and trinuclear helical complexes by increasing the number of donor atoms in py-hz ligands using bipyridine or terpyridine units. There are many examples of bipyridine-based py-hz ligands that form double helicates with Cu(I), Ni(II), or Zn(II) ions.[5] However, reports of single-stranded helicates with py-hz ligands are less common as they are with other ligand systems,[2, 6] where they often represent a single example.[7] Single-stranded helicates are attractive for generating reversible metal-induced molecular machines because the metal ions reside on the exterior of the ligand and can be more easily accessed by sequestering ligands. While the conditions for double and triple helicate formation are now well-known,[6] the factors governing single helicate formation are not as certain. This is partly due to the difficulty in predicting how the empty coordination sites in single helicates will interact with secondary or ancillary ligands. Some promising strategies to single helicates include *cis*-protecting Pd(II) and Ru(II) ions so that ligands coordinate to only one hemisphere of the metal ion,[8] condensing pre-formed square planar templates so that the coordination sphere of the metal ions is fixed,[7f] and using Ag⋯Ag interactions to favour coordination of metal ions within a single ligand.[7c] Although the protecting groups are essential for the assembly of single-stranded helicates in many of these examples, they ultimately detract from the single helical appearance of the complexes.[9]

One strategy to synthesise highly-saturated single-stranded helicates exploits the high coordination number and diverse geometries of Pb^{II}. The reaction of a terpyridine-based py-hz ligand with Pb^{II} produces a saturated dinuclear single-stranded helicate with the metals ions accommodated in discrete coordination sites on the ligand.[10] The high denticity of the py-hz ligands ensures that the Pb^{II} ions are saturated by the helical ligand rather than by mono- or bidentate ancillary ligands from solution. All that is required of the ligand is to contain a sufficiently high number of donor atoms to twist down and around the Pb^{II} ions in the identical absolute configurations of a helicate. The stereochemically-active lone pair in Pb^{II} can further favour saturated single-stranded helicates by occupying a site on the metal ion where a second ligand may coordinate in a double helicate.[11]

In the study reported herein, a series of modifed py-hz ligands (**L1**-**L5**) with different numbers of donor atoms were made. The ligands were modified with hydroxymethyl and acryloyl substituents to allow their incorporation into polymer gels but the functional groups could also participate in coordination with Pb^{II}. Previous studies of hydroxymethyl-terminated pyrimidine-hydrazones have shown that binding of the oxygen donors alongside the pyrimidine-hydrazone chelates distort the geometries of Pb^{II} grid complexes.[12] The hydroxymethyl groups

[a] *M. L. Lobo, Associate Professor S. C. Moratti, Professor L. R. Hanton*
Department of Chemistry
University of Otago
PO Box 56, Dunedin, New Zealand
E-mail: lhanton@chemistry.otago.ac.nz

Supporting information for this article is given via a link at the end of the document.

Accepted Manuscript

This article is protected by copyright. All rights reserved.

10.1002/asia.201801784

in these py-hz ligands are unlikely to impede the assembly of single-stranded Pb^{II} helicates since such structures inherently have no geometry restrictions.

Results and Discussion

The pyridine amine precursors **3** and **4** were synthesised by reaction of 6-bromo-3-(hydroxymethyl)pyridine or 6-bromo-2-(hydroxymethyl)pyridine with a large excess of methylhydrazine and purified by washing the reaction mixture with a dilute solution of Na_2CO_3 and extraction with high polarity 3:1 $CHCl_3$/*i*PrOH mixtures. The terpyridine amine **6** was synthesised by aldol condensation of 2-acetyl-6-bromopyridine with benzaldehyde then reaction with methylhydrazine. The pyridine aldehyde precursors **1** and **2** were prepared by oxidation of 2,6-pyridinedimethanol using stoichiometric equivalents of SeO_2.

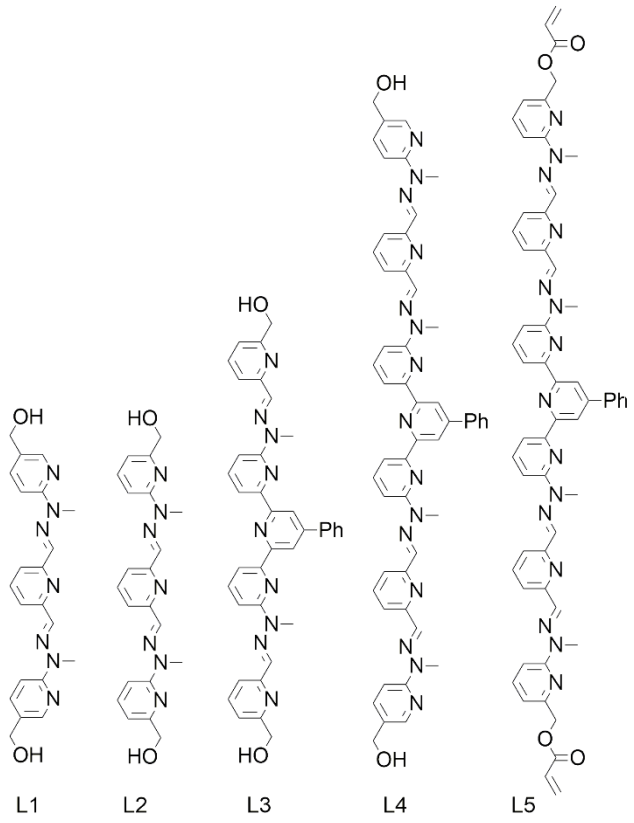

Figure 1. Pyridine-hydrazone ligands **L1**-**L5**.

The reaction of **1** with two equivalents of **3** or **4** in refluxing ethanol resulted in the precipitation of **L1** and **L2**, respectively. **L1** could be sparingly dissolved in DMSO for NMR spectroscopy. The lack of correlations in the NOESY spectrum of **L1** indicated the molecule most likely had a linear shape. **L3** was synthesised by the reaction of **6** with two equivalents of **2** and isolated as a yellow solid by filtration of the reaction mixture. **L3** could not be solubilised in sufficient quantities for NMR spectroscopy. However, the NOESY spectrum of a soluble acryloyl-modified derivative of **L3** was consistent with a linear shape in solution. A convergent method was used to prepare **L4** because it reduced the number of reactive ends that could lead to polymeric molecules.[13] In this method, **1** and **3** were first reacted together in a 1:1 molar ratio to synthesise the difunctional aldehyde **7** then **7** reacted with **6** to form **L4**. The py-hz ligand **L5** was prepared in a similar way to **L4** by the reaction of **6** with two equivalents of **9**. Both **L4** and **L5** were insoluble in organic solvents so proof of their syntheses relied mainly on IR spectroscopy, elemental analysis, and the Pb^{II} complexes they formed. A diagram of the ligands **L1**-**L5** is shown in **Error! Reference source not found.**.

Mononuclear Pb^{II} Complex of L1. The high coordination tendencies of Pb^{II} directed mononuclear complexes with **L1**. When **L1** was stirred with two equivalents of $Pb(CF_3SO_3)_2{\cdot}H_2O$ in CH_3CN, the orange solid that precipitated from the solution upon vapour diffusion of Et_2O had elemental analysis that was consistent with an empirical formula of Pb**L1**$(CF_3SO_3)_2$. There were correlations between protons H3 and H5 as well as H8 and H14 in the NOESY spectrum of Pb**L1**$(CF_3SO_3)_2$ that indicated all the nitrogen donors were likely coordinated to Pb^{II} in a mononuclear complex (Figure 2).

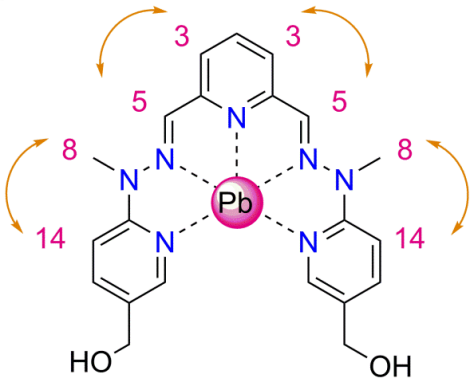

Figure 2. Solution structure of Pb**L1**$(CF_3SO_3)_2$ (NMR numbering) with NOE correlations indicated by double-sided arrows.

Crystal Structure of [PbL1$(CF_3SO_3)_2$]·$CHCl_3$. The mononuclear complex had C_2 symmetry in solution but existed as a centrosymmetric dimer in the solid-state through bridging of one of the hydroxymethyl O2 donors (Figure 3). The mononuclear complex crystallised in the *P*-1 space group with one [Pb**L1**$(CF_3SO_3)_2$]·$CHCl_3$ moiety in the asymmetric unit. The seven-coordinated Pb1 had a pentagonal bipyramidal geometry with five nitrogen donors from the ligand, one axial CF_3SO_3 anion, and one bridging O2 donor (Figure 4). Pb^{II} could accommodate all the nitrogen donors in the ligand to give a highly-planar mononuclear complex.

Accepted Manuscript

This article is protected by copyright. All rights reserved.

10.1002/asia.201801784

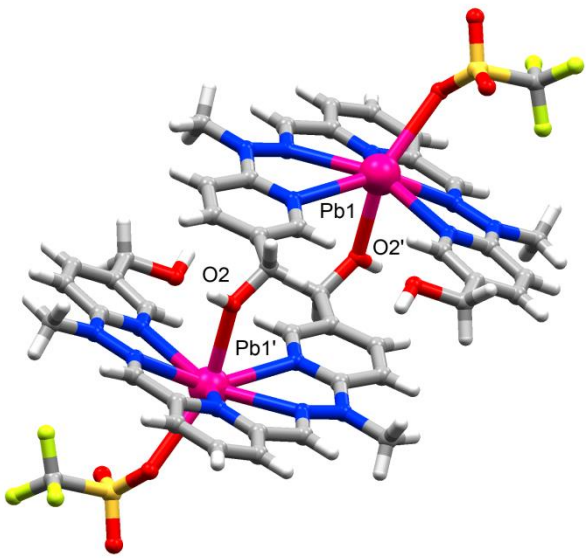

Figure 3. Crystal structure of [Pb**L1**CF_3SO_3]$^+$ showing centrosymmetric dimer.

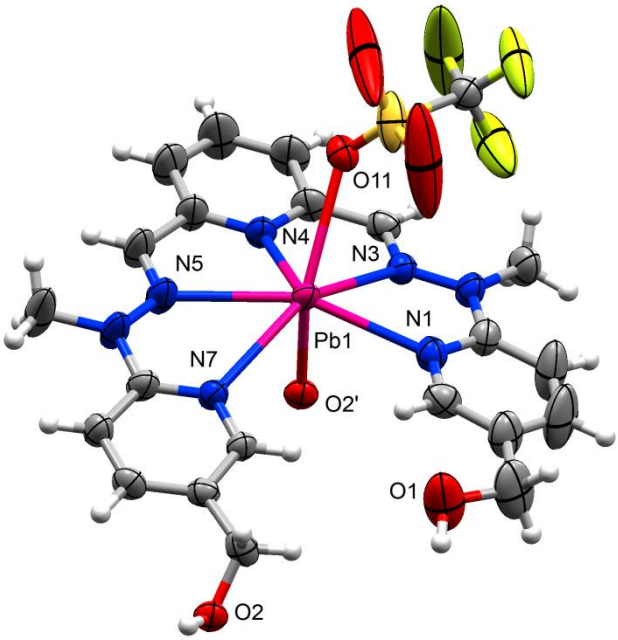

Figure 4. Crystal structure of [Pb**L1**CF_3SO_3]$^+$ moiety with thermal ellipsoids shown at 50% probability level.

Mononuclear Pb^{II} Complex of L2. The next ligand **L2** had an identical arrangement of nitrogen donors as **L1** but the hydroxymethyl donors could coordinate to Pb^{II}. The solid that precipitated from the reaction of **L2** with two equivalents of $Pb(CF_3SO_3)_2{\cdot}H_2O$ had elemental analysis consistent with an empirical formula of Pb**L2**$(CF_3SO_3)_2$. There were correlations between protons H3 and H5 as well as H8 and H14 in the NOESY spectrum of Pb**L2**$(CF_3SO_3)_2$ that indicated all the nitrogen donors were likely coordinated in a mononuclear Pb^{II} complex (Figure 5).

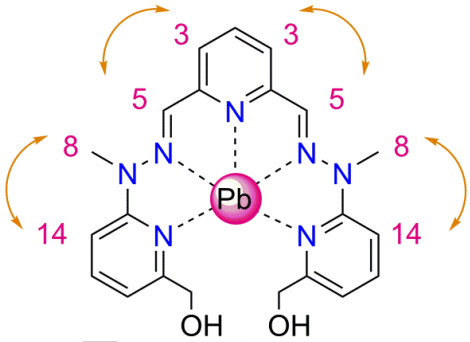

Figure 5. Solution structure of Pb**L2**$(CF_3SO_3)_2$ (NMR numbering) with NOE correlations indicated by double-sided arrows.

Crystal Structure of PbL2$(CF_3SO_3)_2$][PbL2CF_3SO_3]$CF_3SO_3{\cdot}CH_3CN$. The mononuclear complex crystallised in the $P2_1/c$ space group with a Pb**L2**$(CF_3SO_3)_2$][Pb**L2**CF_3SO_3]$CF_3SO_3{\cdot}CH_3CN$ moiety in the asymmetric unit. The two molecules in the asymmetric unit spanned the high coordination possibilities of Pb^{II} with Pb1 in a nine-coordinate environment consisting of the heptadentate ligand and two CF_3SO_3 anions and Pb2 in an eight-coordinate environment comprised of the ligand and one CF_3SO_3 anion (Figure 6). The increased denticity of **L2** produced considerable twists in the ligand to accommodate the Pb-O bonds above and below the complex. These non-planar mononuclear Pb^{II} complexes of **L2** could be considered mono-helical precursors and indicate the possibility of single-stranded helicate formation with the longer-stranded py-hz ligands.

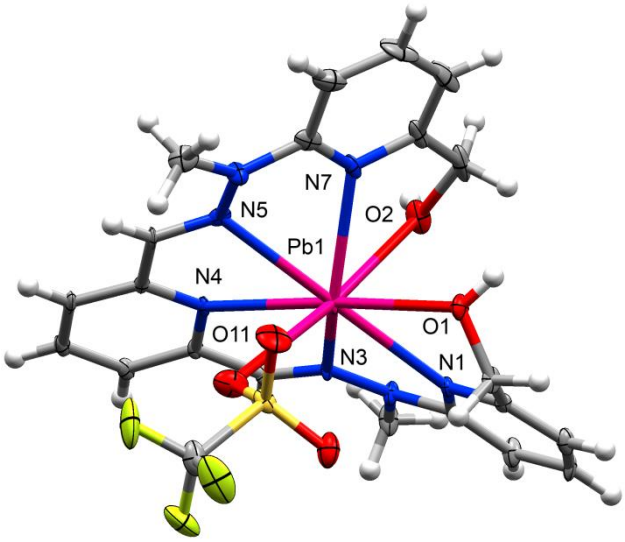

Accepted Manuscript

This article is protected by copyright. All rights reserved.

10.1002/asia.201801784

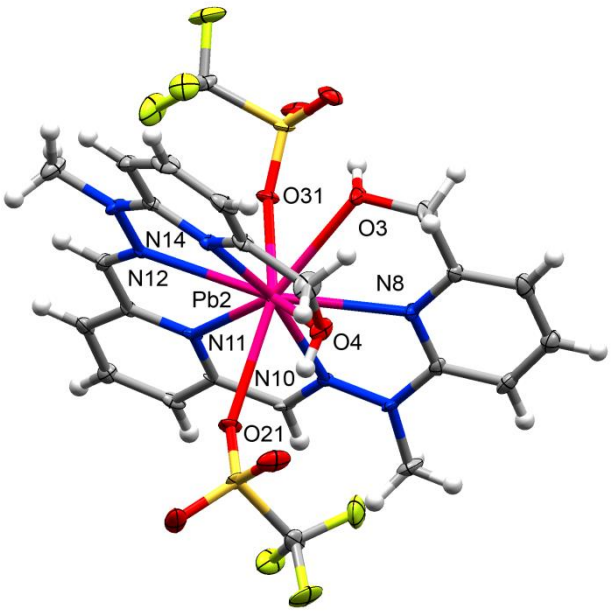

Figure 6. Crystal structures of [Pb**L2**(CF_3SO_3)]$^+$ and [Pb**L2**(CF_3SO_3)$_2$] moieties with thermal ellipsoids shown at 50% probability level.

***Meso*-Helical Pb^{II} Complex of L3**. An increase in the number of donor atoms in the py-hz ligand **L3** directed dinuclear single-stranded *meso*-helicates with Pb^{II}. The reaction of **L3** with four equivalents of Pb(CF_3SO_3)$_2$·H_2O produced a yellow solution, from which an orange solid was precipitated by vapour diffusion of Et_2O. Electrospray mass spectrometry of Pb_2**L3**(CF_3SO_3)$_4$ showed ions due to dinuclear Pb^{II} complexes with ionic composition of [**L3**+Pb_2+CF_3SO_3-H]$^{2+}$. The electrospray mass spectrum also showed that the ligand had abstracted bromide anions in Pb^{II} complexes of [**L3**+Pb_2+Br-H]$^{2+}$. The correlations between protons H3 and H10, H8 and H16 as well as H18 and H24 in the NOESY spectrum of Pb_2**L3**(CF_3SO_3)$_4$ indicated that the dinuclear Pb^{II} complex was symmetrical in solution (Figure 7). In addition, the equivalency of the methylene protons in the ^{1}H NMR spectrum indicated that the symmetrical complex was achiral. The lack of chirality in this dinuclear complex was subsequently confirmed by a crystal structure, which showed a *meso*-helicate (Figure 8).

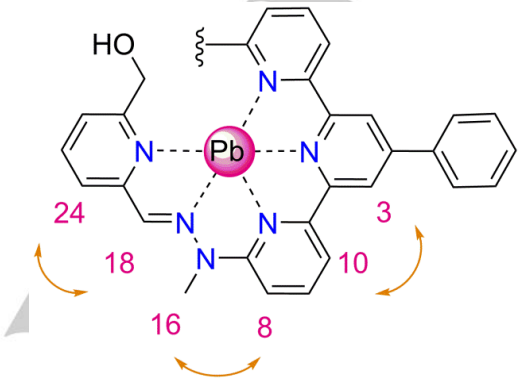

Figure 7. Solution structure of Pb_2**L3**(CF_3SO_3)$_4$ (NMR numbering) with NOE correlations indicated by double-sided arrows.

Crystal Structure of [Pb_2L3(CF_3SO_3)$_2$Br]CF_3SO_3·CH_3CN. The dinuclear *meso*-helicate crystallised in the $P2_1/c$ space group with one [Pb_2**L3**(CF_3SO_3)$_2$Br]CF_3SO_3·CH_3CN moiety in the asymmetric unit. The twisting of **L3** into a half-a-helical turn around the two Pb^{II} ions resulted in a *meso*-helicate with the metal ions in opposite absolute configurations (Figure 9). The conformation of the ligand in the *meso*-helicate provided a cleft that was ideal for the abstraction of bromide anions from solution during crystallisation. This bromide anion was bridged between Pb1 and Pb2 [Pb1-Br1 3.016(3) Å and Br1-Pb2 2.916(3) Å]. The bridging of ancillary hydroxide and nitrate donors across metal ions has also been observed in the *meso*-helicates of other py-hz ligands.[14] Pb1 was in a seven-coordinate environment consisting of a pentadentate chelate from the ligand, a bridging bromide, and an axial CF_3SO_3 anion. Pb2 was in a lower six-coordinate environment consisting of four nitrogen donors from the ligand, a bridging bromide, and an axial CF_3SO_3 anion. The higher seven-coordinate environment around Pb1 led to a distinctly holohedral distribution around the Pb^{II} ion. In contrast, the hemidirecting influence of the stereochemically-active lone pair in the lower six-coordinate Pb2 was apparent in the large O2-Pb2-N6 [170.3(4)°] angle and long distance between Pb2 and N5 [2.997(15) Å]. This stereochemically-active lone pair occupied the coordination sites in Pb2 where a second ligand may have coordinated in a double helicate.

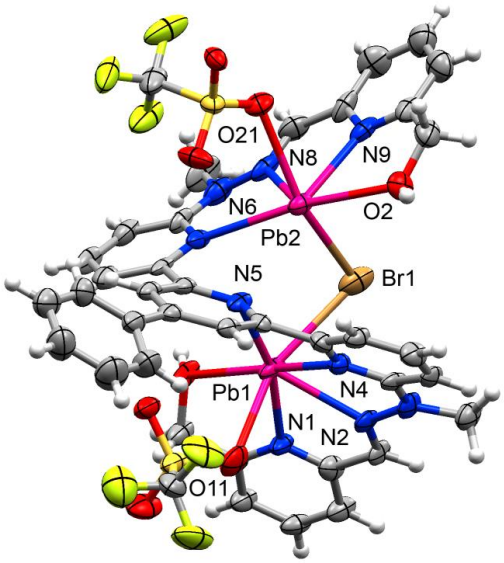

Figure 8. Crystal structure of [Pb_2**L3**(CF_3SO_3)$_2$Br]$^+$ moiety with thermal ellipsoids shown at 50% probability level.

Accepted Manuscript

This article is protected by copyright. All rights reserved.

10.1002/asia.201801784

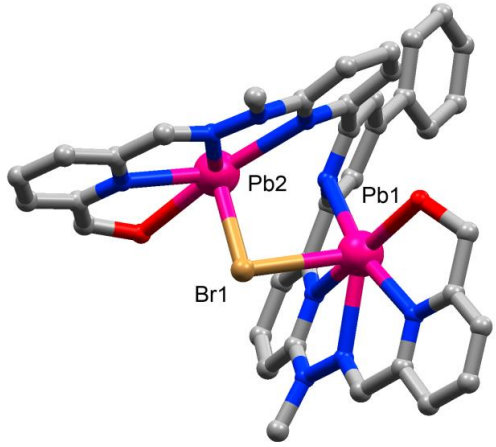

Figure 9. Ball-and-stick model of crystal structure of $[Pb_2\mathbf{L3}]^{4+}$ moiety showing the *meso*-helical shape of complex.

Single Helical Pb^{II} Complexes of L4. The ligand **L4** contained a sufficiently high number of donor atoms to direct single helicates with Pb^{II}. The solid that precipitated from the reaction of **L4** with five equivalents of $Pb(CF_3SO_3)_2{\cdot}H_2O$ in CH_3CN had elemental analysis consistent with an empirical formula of $Pb_2\mathbf{L4}(CF_3SO_3)_4$. The single helical structure of the complex was confirmed by ^{1}H NMR spectroscopy, which showed an upfield shifting of the H8 and H31 signals due to shielding between the helically-twisted ligand. The single helicate was also characterised by the splitting of the hydroxymethyl protons into an AB multiplet in the ^{1}H NMR spectrum. The NOESY spectrum of $Pb_2\mathbf{L4}(CF_3SO_3)_4$ showed correlations between protons H3 and H10; H8 and H16; H18 and H24; and H28 and H34 (Figure 10) that indicated the Pb^{II} ions were identically coordinated in the single helicate.

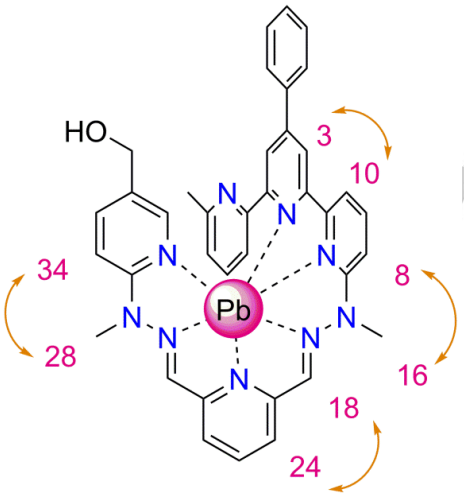

Figure 10. Solution structure of $Pb_2\mathbf{L4}(CF_3SO_3)_4$ (NMR numbering) with NOE correlations indicated by double-sided arrows.

Crystal Structure of $[Pb_2L4(CF_3SO_3)_3]CF_3SO_3{\cdot}CH_3CN$. Crystals of the dinuclear single helicate were obtained by vapour diffusion of Et_2O into a solution of **L4** and five equivalents of $Pb(CF_3SO_3)_2{\cdot}H_2O$ in CH_3CN (Figure 11). The complex crystallised in the *P*-1 space group with one $[Pb_2\mathbf{L4}(CF_3SO_3)_3]CF_3SO_3{\cdot}CH_3CN$ moiety in the asymmetric unit. The coordination of Pb1 to six donors of **L4** and one CF_3SO_3 anion placed it in a higher seven-coordinate environment than the six-coordinate Pb2, which was coordinated to only four donors of **L4** and two axial CF_3SO_3 anions. The large number of donor atoms in **L4** allowed it to coordinate to the two Pb^{II} ions in the identical absolute configuration of a single-stranded helicate. The high denticity of **L4** in the single helicate also ensured that more than 2/3 of the coordination spheres of the Pb^{II} ions were saturated by the helical ligand rather than CF_3SO_3 anions.

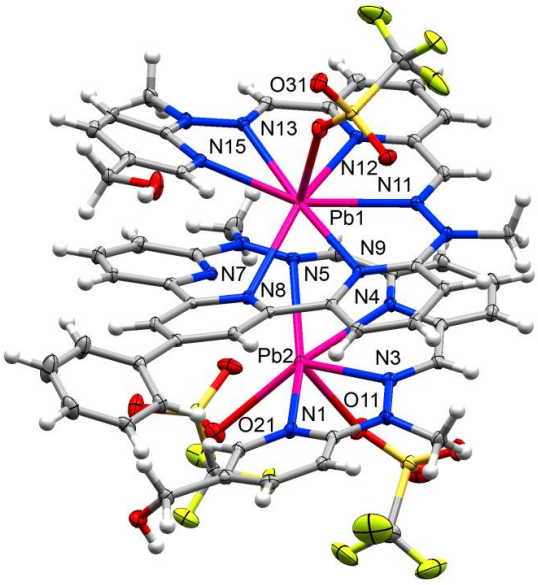

Figure 11. Crystal structure of $[Pb_2L4(CF_3SO_3)_3]^+$ moiety with thermal ellipsoids shown at 50% probability level.

Crystal Structure of $[Pb_2L4CF_3SO_3(CH_3OH)_2](CF_3SO_3)_3{\cdot}2CH_3OH{\cdot}2H_2O$. A second set of crystals of the dinuclear single helicate were obtained by vapour diffusion of Et_2O into a solution of **L4** and five equivalents of $Pb(CF_3SO_3)_2{\cdot}H_2O$ in CH_3OH. The complex crystallised in the $P2_1/n$ space group with a $[Pb_2\mathbf{L4}CF_3SO_3(CH_3OH)_2](CF_3SO_3)_3{\cdot}2CH_3OH{\cdot}2H_2O$ moiety in the asymmetric unit (Figure 12). Pb1 was in a nine-coordinate environment consisting of a heptadentate nitrogen chelate from **L4** and two oxygen donors from a CF_3SO_3 anion. Pb2 shared a nitrogen donor (N8) with Pb1 [Pb1-N8 2.791(7) Å and Pb2-N8 2.905(8) Å] so that it was in a seven-coordinate environment consisting of a pentadentate nitrogen chelate from **L4** and two monodentate CH_3OH donors. It is interesting that both these Pb^{II} single helicates, as well as the one example in the literature,[10] are limited to three ancillary ligands in the crystal structure despite

Accepted Manuscript

This article is protected by copyright. All rights reserved.

10.1002/asia.201801784

differing in the types and denticities of the donor atoms. The close resemblance of all these complexes indicates the reliability of generating single helicates from py-hz ligands and Pb^{II}.

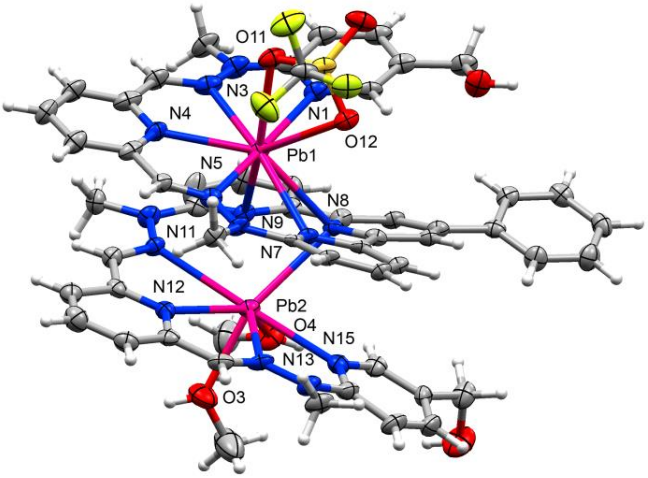

Figure 12. Crystal structure of $[Pb_2\mathbf{L4}CF_3SO_3(CH_3OH)_2]^{3+}$ moiety with thermal ellipsoids shown at 50% probability level.

Pb^{II} Complexes of L5. The ligand **L5** had a similar donor set to the previous ligand **L4** except that the terminal pyridine rings were substituted with acryloyl groups. Reaction of **L5** with five equivalents of $Pb(CF_3SO_3)_2.H_2O$ led to a yellow solution, from which an orange solid was isolated by vapour diffusion of Et_2O. The elemental analysis of the solid indicated a mixture of different Pb^{II} complexes was likely present. When the complexation of **L5** with $Pb(CF_3SO_3)_2{\cdot}H_2O$ was studied using ^1H NMR spectroscopy, the evolution of helical and non-helical Pb^{II} complexes was observable in the ^1H NMR spectra (Figure 13). At one equivalent of Pb^{II}, a single helicate was present in solution that was characterised by a splitting of the methylene protons (H35) into an AB quartet (J = 13.7 Hz) as well as upfield shifts of many of the aromatic protons. Between one and two equivalents of Pb^{II}, the helicates had rearranged into a mixture of non-helical complexes. This mixture of complexes was characterized by the broadening of the methylene protons (H35) in the ^1H NMR spectrum. An increase in the equivalents of Pb^{II} from two to eight resulted in the progressive broadening of some aromatic signals in the ^1H NMR spectra and steady sharpening of others. The broadening of the H16 signal at lower equivalents of Pb^{II} indicated that the terpyridine unit in **L5** had significantly different coordination modes between the helical and non-helical complexes.

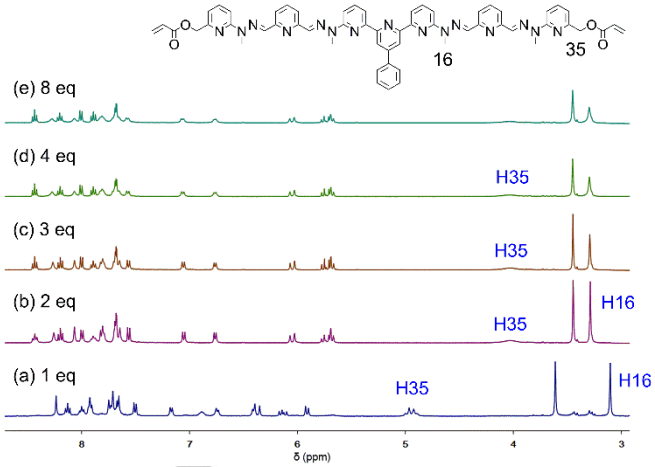

Figure 13. ^1H NMR spectra of **L5** with a) one, b) two, c) three, d) four, e) eight equivalents of $Pb(CF_3SO_3)_2{\cdot}H_2O$ in CD_3CN.

Crystal Structure of $[Pb_3L5(CF_3SO_3)_5]CF_3SO_3{\cdot}3CH_3CN{\cdot}Et_2O$. One of the many Pb^{II} complexes in solution may have included a non-helical trinuclear Pb^{II} complex of **L5**. Crystals of a trinuclear Pb^{II} complex were isolated from the bulk mixture in CD_3CN by vapour diffusion of Et_2O (Figure 14). The complex crystallised in the $P2_1/n$ space group with one $[Pb_3\mathbf{L5}(CF_3SO_3)_5]CF_3SO_3{\cdot}3CH_3CN{\cdot}Et_2O$ moiety in the asymmetric unit. Pb1 and Pb3 had identical donor sets consisting of a tetradentate chelate from the ligand, one monodentate CF_3SO_3, and a bridging bidentate CF_3SO_3 anion. Pb2 was in a five-coordinate environment consisting of a tridentate terpyridine unit from the ligand and two CF_3SO_3 anions. Both Pb1 and Pb3 had large angles [N1-Pb1-N5 155.50(11)° and N11-Pb3-N15 156.99(11)°] in their coordination spheres that may be considered evidence for stereochemically-active lone pairs but could also be unusable coordination sites due to the steric bulk of **L5**. These vacant coordination sites were especially too small for the bulky acryloyl donors, which instead remained oriented outwards from the complex (Figure 15). If the acryloyl groups had coordinated to Pb^{II}, this trinuclear complex might have been destabilised in favour of the single-stranded helical complex found in solution.

Accepted Manuscript

This article is protected by copyright. All rights reserved.

10.1002/asia.201801784

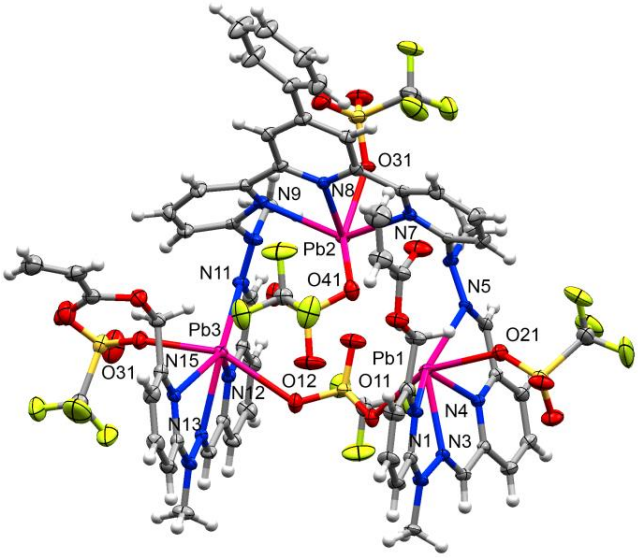

Figure 14. Crystal structure of $[Pb_3\mathbf{L5}(CF_3SO_3)_5]^+$ moiety with thermal ellipsoids shown at 50% probability level.

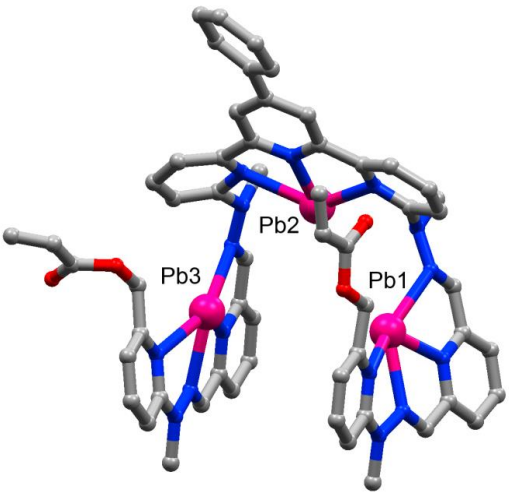

Figure 15. Ball-and-stick model of crystal structure of $[Pb_3\mathbf{L5}]^{6+}$ moiety showing the non-helical shape of complex.

Conclusions

This paper describes some rare examples of discrete single helical Pb^{II} complexes using related ligand systems. The high coordination number of Pb^{II} with **L1** and **L2** directed non-helical mononuclear complexes. However, an increase in the number of donor atoms in **L3** allowed dinuclear single-stranded helical complexes to form. The dinuclear *meso*-helicates of **L3** had stereochemically-active lone pairs on Pb^{II} that prevented the coordination of a second ligand in a double helicate. However, **L3** did not contain enough donor atoms to direct a single helicate with Pb^{II}. Only **L4** contained a sufficiently high number of donor atoms to coordinate around two Pb^{II} ions in the identical absolute configurations of a single helicate. The high denticity of **L4** in the single helicates ensured that the Pb^{II} ions were mostly saturated by the helical ligands rather than ancillary CF_3SO_3 or CH_3OH donors. The contraction of py-hz ligands between the uncoordinated and *meso*-helical and single-helical states is promising but the complicated coordination of the acryloyl-modified **L5** to Pb^{II} will need to be considered in the future design of dynamic polymer gels.

Experimental Section

General. All chemicals were used as received without further purification. $Pb(CF_3SO_3)_2{\cdot}H_2O$ was synthesized by treatment of $PbCO_3{\cdot}Pb(OH)_2$ with HCF_3SO_3. All reaction solvents except EtOH were AR grade or higher. PE was of the 40/60 variety. Dry CH_2Cl_2 was obtained from a Pure Solv MD-6 solvent purification system. ^{1}H NMR, ^{13}C NMR, COSY, NOESY, ROESY, HSQC, and HMBC spectra were collected on 400 or 500 MHz Varian UNITY INOVA spectrometers at 298 K. The ^{1}H NMR and ^{13}C NMR chemical shifts were referenced to the residual non-perdeuterated solvent as reported by Gottlieb.[15] The order of signal assignment in NMR spectra is as follows: chemical shift, multiplicity, coupling constant(s), number of protons, and assignment. Multiplicities are reported with the following notations s (singlet), d (doublet), t (triplet), dd (doublet of doublets), dt (doublet of triplets), dq (doublet of quartets), td (triplet of doublets), m (multiplet). IR spectra were recorded on a Bruker Optics Alpha FT-IR spectrometer with a diamond ATR top-plate. Microanalyses were determined at the Campbell Microanalytic Laboratory University of Otago using a Carlo Erba 1108 CHNS combustion analyser. HR-ESI-MS were run on a Bruker microTOFQ instrument with ESI source in a positive or negative mode.

X-ray Crystallography. Single crystals were mounted in paratone-N oil on a nylon loop. Data were collected on an Agilent Technologies Supernova system at 100 K at the University of Otago using mirror monochromated Mo *K*α (λ = 0.71073 Å) or Cu *K*α (λ = 1.54184 Å) radiation. The data were treated using CrysAlisPro.[16] Intensities were corrected for Lorentz polarisation effects,[17] and a multiscan absorption correction applied.[18] The structures were solved by direct methods (SHELXT[19] or SIR-97[20]) and refined on F^2 using all data by full-matrix least-squares procedures in SHELXL-2014[21] within the WINGX[22] interface. Detailed analyses of the extended structures were carried out using PLATON[23] and MERCURY[24] (Version 3.9).

2,6-Pyridinedicarboxaldehyde (1). A mixture of 2,6-pyridinedimethanol (2.02 g, 14.5 mmol) and SeO_2 (3.22 g, 29.0 mmol) in $CHCl_3$ (120 mL) was heated at reflux for 24 h. The mixture was cooled to RT, filtered, and the filtrate evaporated *in vacuo* to an orange solid. The orange solid was purified through celite with CH_2Cl_2 (100 mL) to give **1** (1.72 g, 12.7 mmol, 88%) as an off-white solid.[25] ^{1}H NMR (400 MHz, [D]chloroform) δ 10.17 (d, J = 0.8 Hz, 1H, H-5), 8.18 (dd, J = 7.7, 0.8 Hz, 1H, H-3), 8.08 (m, 1H, H-4) ppm. ^{13}C NMR (100 MHz, [D]chloroform): δ 192.4 (C-5), 152.9 (C-2), 138.4 (C-4), 125.3 (C-3) ppm. Selected IR ν/cm^{-1}: 3085 (sh, wk, C-H), 3018 (sh, wk), 2922 (sh, wk), 2858 (sh, md), 1715 (sh, str, C=O), 1692 (sh, str), 1579 (sh, wk), 1348 (sh, str), 1300 (sh, wk), 1259 (sh, str), 1226 (sh, str), 1164 (sh, wk), 1086 (sh, wk).

6-Hydroxymethyl-2-pyridinecarboxaldehyde (2). A mixture of 2,6-pyridinedimethanol (2.06 g, 14.8 mmol) and SeO_2 (0.832 g, 7.49 mmol) in $CHCl_3$ (200 mL) was heated at reflux for 16 h. The mixture was cooled to RT, filtered, and the filtrate evaporated *in vacuo* to a yellow oil. The yellow oil was purified by column chromatography on silica gel eluted with a

Accepted Manuscript

This article is protected by copyright. All rights reserved.

gradient of EtOAc/CH_2Cl_2 (0 to 100%) to give **2** (1.22 g, 8.89 mmol, 60%) as a yellow oil that solidified on standing.[26] ^{1}H NMR (400 MHz, [D]chloroform): *δ* 10.09 (s, 1H, H-8), 7.89 (m, 2H, H-3/5), 7.52 (m, 1H, H-4), 4.88 (s, 2H, H-7) ppm. ^{13}C NMR (100 MHz, [D]chloroform): *δ* 193.2 (C-8), 160.2, 151.8, 137.9, 124.9, 120.6, 64.2 (C-7) ppm. Selected IR v/cm^{-1}: 3134 (br, md, O-H), 2841 (br, wk), 2719 (br, wk), 1708 (sh, md, C=O), 1599 (sh, md), 1449 (sh, md), 1336 (sh, md), 1267 (sh, wk), 1210 (sh, md), 1144 (sh, wk), 1103 (sh, str), 1043 (sh, str).

3-(Hydroxymethyl)6-(1-methylhydrazino)pyridine (3). Methylhydrazine (3.00 mL, 57.0 mmol) was added to 6-bromo-3-(hydroxymethyl)pyridine (1.02 g, 5.42 mmol) and the solution heated at reflux for 24 h under an Ar atmosphere. The solution was cooled to RT then extracted with 3:1 $CHCl_3$/*i*PrOH, washed with 5% Na_2CO_3, extracted with 3:1 $CHCl_3$/*i*PrOH and evaporated *in vacuo* to give **3** (0.810 g, 5.29 mmol, 97%) as an opaque oil. ^{1}H NMR (400 MHz, [D]chloroform): *δ* 8.12 (d, *J* = 2.4 Hz, 1H, H-6), 7.53 (dd, *J* = 8.7, 2.4 Hz, 1H, H-4), 6.96 (dd, *J* = 8.8, 0.8 Hz, 1H, H-3), 4.57 (s, 2H, H-7), 3.28 (s, 3H, H-8) ppm. ^{13}C NMR (100 MHz, [D]chloroform): *δ* 161.1 (C-2), 144.5(C-6), 139.9 (C-4), 126.8 (C-5), 109.5 (C-3), 62.3 (C-7), 41.2 (C-8) ppm. HR-ESI-MS: Calcd for [**3**+H]$^+$ ($C_7H_{12}N_3O$) *m/z* 154.0975; Found. 154.0963.

2-(Hydroxymethyl)6-(1-methylhydrazino)pyridine (4). Methylhydrazine (3.00 mL, 57.0 mmol) was added to 6-bromo-2-(hydroxymethyl)pyridine (0.923 g, 4.91 mmol) and the solution heated at reflux for 23 h under an Ar atmosphere. The solution was cooled to RT then extracted with 3:1 $CHCl_3$/*i*PrOH, washed with 5% Na_2CO_3, extracted with 3:1 $CHCl_3$/*i*PrOH and evaporated *in vacuo* to give **4** as an opaque oil (0.689 g, 4.49 mmol, 92%). ^{1}H NMR (400 MHz, [D]chloroform): *δ* 7.47 (dd, *J* = 8.4, 7.3 Hz, 1H, H-4), 6.85 (dq, *J* = 8.4, 0.7 Hz, 1H, H-5), 6.50 (dq, *J* = 7.3, 0.8 Hz, 1H, H-3), 4.62 (t, *J* = 0.7 Hz, 2H, H-7), 3.30 (s, 3H, H-8) ppm. ^{13}C NMR (100 MHz, [D]chloroform): *δ* 160.6 (C-2/6), 156.6 (C-2/6), 138.1 (C-3/4/5), 108.9 (C-3/4/5), 105.7 (C-3/4/5), 63.8 (C-7), 41.2 (C-8) ppm. HR-ESI-MS: Calcd for [**4**+Na]$^+$ ($C_7H_{11}N_3NaO$) *m/z* 176.0794; Found. 176.0790.

6,6''-Dibromo-4'-phenyl-2,2':6',2''-terpyridine (5). 2-Acetyl-6-bromopyridine (2.55 g, 12.7 mmol) was added to a solution of KOH (2.94 g, 52.5 mmol) in dry EtOH (40 mL) and the solution stirred for 30 min under an Ar atmosphere. Benzaldehyde (0.650 mL, 6.40 mmol) and NH_3 (2M in EtOH) (10.0 mL, 20.0 mmol) were added and the orange solution stirred at RT for 25 h under an Ar atmosphere. The white precipitate was filtered, washed with EtOH then dried under vacuum to give **5** (1.86 g, 3.99 mmol, 31%) as a white solid.[27] ^{1}H NMR (500 MHz, [D]chloroform): *δ* 8.70 (s, 2H, H-3), 8.59 (dd, *J* = 7.7, 0.9 Hz, 2H, H-8), 7.87 (m, 2H, H-12), 7.72 (t, *J* = 7.8 Hz, 2H, H-9), 7.54 (m, 4H, H10/13), 7.49 (m, 1H, H-14) ppm. ^{13}C NMR (126 MHz, [D]chloroform): *δ* 157.4 (C-5), 154.5 (C-2), 151.0 (C-11), 141.8 (C-7), 139.3 (C-9), 138.3 (C-4), 129.4 (C-14), 129.2 (C-13), 128.4 (C-10), 127.6 (C-12), 120.2 (C-8), 120.1 (C-3) ppm. Selected IR *v*/cm^{-1}: 1603 (sh, wk), 1576 (sh, str), 1541 (sh, str), 1497 (sh, md), 1455 (sh, md), 1437 (sh, str), 1388 (sh, str), 1162 (sh, wk), 1150 (sh, md), 1121 (sh, str), 1072 (sh, md), 1058 (sh, md). HR-ESI-MS: Calcd for [**5**+Na]$^+$ ($C_{21}H_{13}Br_2N_3Na$) *m/z* 489.9353; Found. 489.9321. Elemental analysis calcd for $C_{21}H_{13}Br_2N_3$: C, 53.99; H, 2.81; N, 8.99. Found: C, 53.86; H, 2.86; N, 8.72.

6,6''-Bis(1-methylhydrazino)-4'-phenyl-2,2':6',2''-terpyridine (6). Methylhydrazine (5.00 mL, 95.0 mmol) was added to **5** (0.524 g, 1.12 mmol) and the mixture heated at reflux for 23 h under an Ar atmosphere. The yellow mixture was cooled to RT, extracted with CH_2Cl_2, washed with 10% Na_2CO_3, extracted with CH_2Cl_2, washed with water, dried with Na_2SO_4 and evaporated *in vacuo* to give **6** (0.430 g, 1.08 mmol, 96%) as a yellow solid. ^{1}H NMR (500 MHz, [D]chloroform): *δ* 8.60 (s, 2H, H-3), 8.03 (dd, *J* = 7.4, 0.8 Hz, 2H, H-10), 7.82 (m, 2H, H-12), 7.68 (dd, *J* = 8.4, 7.4 Hz, 2H, H-9), 7.54 (m, 2H, H-13), 7.48 (m, 1H, H-14), 7.02 (dd, *J* = 8.4, 0.8 Hz, 2H, H-8), 3.39 (s, 6H, H-16) ppm. ^{13}C NMR (126 MHz, [D]chloroform): *δ* 160.9 (C-7), 156.4 (C-3), 153.9 (C-5), 149.9 (C-11), 139.7 (C-4), 138.3 (C-9), 129.2 (C-13), 128.9 (C-14), 127.4 (C-12), 118.6 (C-3), 110.9 (C-10), 107.9 (C-8), 41.4 (C-15) ppm. Selected IR *v*/cm^{-1}: 3304 (sh, wk, N-H), 1641 (sh, md), 1578 (sh, str), 1560 (sh, str), 1542 (sh, str), 1469 (sh, md), 1394 (sh, str), 1289 (sh, md), 1233 (sh, md), 1121 (sh, md). HR-ESI-MS: Calcd for [**6**+H]$^+$ ($C_{23}H_{24}N_7$) *m/z* 398.2093; Found. 398.2096.

Pyridine-2-carboxaldehyde-(5-hydroxymethyl-pyridine-2-yl)methylhydrazone (7). A solution of **3** (0.810 g, 5.29 mmol) in EtOH (100 mL) was added dropwise to a solution of **1** (0.797 g, 5.89 mmol) in EtOH (50 mL) over 1 h and the mixture stirred at RT for 3 h. The yellow mixture was filtered and the filtrate evaporated *in vacuo* to an orange solid. The orange solid was purified by column chromatography on silica gel eluted with a gradient of EtOAc/CH_2Cl_2 (0 to 100%) and CH_3OH/EtOAc (5%) to give **7** (0.581 g, 2.15 mmol, 41%) as a yellow solid. ^{1}H NMR (500 MHz, [D]chloroform) *δ* 10.08 (d, *J* = 0.8 Hz, 1H, H-7), 8.24 (dd, *J* = 7.7, 1.3 Hz, 1H, H-5), 8.22 (dt, *J* = 2.3, 0.8 Hz, 1H, H-14), 7.88 (td, *J* = 7.6, 0.8 Hz, 1H, H-4), 7.85 (m, 1H, H-3), 7.82 (s, 1H, H-8), 7.73 (dt, *J* = 8.7, 0.9 Hz, 1H, H-17), 7.68 (dd, *J* = 8.7, 2.3 Hz, 1H, H-16), 4.66 (s, 2H, H-18), 3.73 (d, *J* = 0.8 Hz, 3H, H-11) ppm. ^{13}C NMR (126 MHz, [D]chloroform): *δ* 193.3 (C-7), 157.1 (C-12), 156.3 (C-6), 152.5 (C-2), 146.2 (C-14), 137.6 (C-16), 137.3 (C-4), 133.7 (C-8), 128.9 (C-15), 123.6 (C-5), 120.9 (C-3), 110.2 (C-17), 62.8 (C-18), 30.2 (C-11) ppm. Selected IR *v*/cm^{-1}: 3263 (br, md, O-H), 2838 (sh, wk, N-H), 1709 (sh, str, C=O), 1605 (sh, str), 1561 (sh, str, C=N), 1483 (sh, str), 1449 (sh, str), 1396 (sh, str), 1319 (sh, str), 1289 (sh, md), 1195 (sh, str), 1146 (sh, md), 1111 (sh, str), 1008 (sh, str). HR-ESI-MS: Calcd for [**7**+Na]$^+$ ($C_{14}H_{14}N_4O_2Na$) *m/z* 293.1015; Found 293.0988. Elemental analysis calcd for $C_{14}H_{14}N_4O_2$: C, 62.21; H, 5.22; N, 20.73. Found: C, 62.45; H, 5.17; N, 20.48.

Pyridine-2-carboxaldehyde-(6-hydroxymethyl-pyridine-2-yl)methylhydrazone (8). A solution of **4** (0.466 g, 3.04 mmol) in $CHCl_3$ (50 mL) was added dropwise to a solution of **1** (0.505 g, 3.74 mmol) in $CHCl_3$ (10 mL) over 2 h and the mixture stirred at RT for 15 h. The yellow mixture was filtered and the filtrate evaporated *in vacuo* to a yellow solid. The solid was purified by column chromatography on silica gel eluted with a gradient of EtOAc/CH_2Cl_2 (0 to 100%) and CH_3OH/EtOAc (0 to 5%) to give **8** (0.361 g, 1.34 mmol, 44%) as a yellow solid. ^{1}H NMR (500 MHz, [D]chloroform) *δ* 10.09 (s, 1H, H-7), 8.25 (dd, *J* = 7.4, 1.6 Hz, 1H, H-5), 7.87 (m, 3H, H-3/4/8), 7.64 (m, 2H, H-15/17), 6.80 (m, 1H, H-16), 4.71 (s, 2H, H-18), 3.75 (s, 3H, H-11) ppm. ^{13}C NMR (126 MHz, [D]chloroform) *δ* 193.3 (C-7), 156.8 (C-14), 156.7 (C-12), 156.2 (C-6), 152.5 (C-2), 138.6 (C-15/17), 137.3 (C-3/4), 134.0 (C-8), 123.6 (C-5), 120.9 (C-3/4), 112.8 (C-16), 108.7 (C-15/17), 64.2 (C-18), 30.1 (C-11) ppm. Selected IR *v*/cm^{-1}: 3256 (br, md O-H), 3076 (sh, wk), 2832 (sh, wk, N-H), 1711 (sh, str, C=O), 1591 (sh, str), 1564 (sh, str, C=N), 1471 (sh, str), 1450 (sh, str), 1418 (sh, str), 1376 (sh, md), 1348 (sh, md), 1314 (sh, md), 1288 (sh, md), 1212 (sh, str), 1153 (sh, md), 1133 (sh, str), 1064 (sh, md), 1027 (sh, md), 1005 (sh, str). HR-ESI-MS: Calcd for [**8**+H]$^+$ ($C_{14}H_{15}N_4O_2$) *m/z* 271.1190; Found 271.1176. Calcd for [**8**+Na]$^+$ ($C_{14}H_{14}N_4NaO_2$) *m/z* 293.1009; Found 293.0994. Elemental analysis calcd for $C_{14}H_{14}N_4O_2$: C, 62.21; H, 5.22; N, 20.73. Found: C, 62.22; H, 5.37; N, 20.43.

Pyridine-2-carboxaldehyde-(6-propenoic acid-pyridine-2-yl)methylhydrazone (9). NEt_3 (0.1 mL, 0.7 mmol) was added to a solution of **8** (0.149 g, 0.551 mmol) in dry CH_2Cl_2 (50 mL) and the solution cooled to 0 °C. Acryloyl chloride (0.05 mL, 0.6 mmol) added and the brown solution stirred at RT for 24 h under an Ar atmosphere. The brown solution was washed with water, washed with $NaHCO_3$, extracted with CH_2Cl_2 and evaporated *in vacuo* to a brown solid. The brown solid was purified by column chromatography on silica gel eluted with a gradient of CH_2Cl_2/PE (50 to 100%) then EtOAc/CH_2Cl_2 (0 to 100%) to give **9** (0.056 g, 0.17 mmol, 31%) as a yellow solid. ^{1}H NMR (400 MHz, [D]chloroform) *δ* 10.08 (s, 1H, H-7), 8.23 (dd, *J* = 7.7, 1.5 Hz, 1H, H-5), 7.87 (m, 1H, H-4), 7.84 (m, 1H, H-3), 7.82 (s, 1H, H-8), 7.65 (m, 2H, H-16/17), 6.90 (dd, *J* = 6.6, 1.6 Hz, 1H, H-15), 6.51 (dd, *J* = 17.3, 1.4 Hz, 1H, H-22a/b), 6.25 (m, 1H, H-21), 5.91 (dd, *J* = 10.5, 1.4 Hz, 1H, H-22a/b), 5.25 (s, 2H, H-18), 3.72 (s, 3H, H-11) ppm. ^{13}C NMR (126 MHz, [D]chloroform) *δ* 166.0 (C-20), 156.9 (C-14), 156.3 (C-12), 153.5 (C-6), 152.5 (C-2), 138.5 (C-16/17), 137.3 (C-4), 133.7 (C-8), 131.5 (C-22), 128.4 (C-21), 123.6 (C-5), 120.9 (C-3), 113.9 (C-15), 109.3 (C-16/17), 66.9 (C-18), 29.9 (C-11) ppm. HR-ESI-MS: Calcd for [**9**+H]$^+$ ($C_{17}H_{17}N_4O_3$) *m/z* 325.1295; Found 325.1308. Calcd for [**9**+Na]$^+$

Accepted Manuscript

This article is protected by copyright. All rights reserved.

($C_{17}H_{16}N_4O_3Na$) *m/z* 347.1115; Found 347.1109. Elemental analysis calcd for $C_{17}H_{16}N_4O_3 \cdot 0.3CH_3COOCH_2CH_3$: C, 62.52; H, 5.19; N, 16.38. Found: C, 62.70; H, 5.20; N, 16.46.

L1. A solution of **3** (1.26 g, 8.22 mmol) and **1** (0.505 g, 3.74 mmol) in EtOH (50 mL) was heated at reflux for 4 h. The yellow mixture was cooled to RT. The yellow precipitate was filtered, washed with EtOH and Et_2O then dried under vacuum to give **L1** (0.833 g, 2.05 mmol, 55%) as a yellow solid. ^{1}H NMR (400 MHz, [D$_6$]DMSO) *δ* 8.18 (dd, *J* = 2.2, 0.9 Hz, 2H, H-11), 7.94 (m, 2H, H-3), 7.86 (dd, *J* = 8.8, 6.8 Hz, 1H, H-4), 7.77 (s, 2H, H-5), 7.74 (dd, *J* = 8.7, 0.9 Hz, 2H, H-13/14), 7.70 (dd, *J* = 8.8, 2.2 Hz, 2H, H-13/14), 4.46 (d, *J* = Hz, 4H, H-15), 3.67 (d, *J* = 0.8 Hz, 6H, H-8) ppm. Selected IR *ν*/cm^{-1}: 3288 (br str, O-H), 3002 (sh, wk, N-H), 2867 (sh, wk, N-H), 1604 (sh, str), 1582 (sh, str), 1562 (sh, str, C=N), 1487 (sh, str), 1455 (sh, str), 1397 (sh, str), 1370 (sh, str), 1311 (sh, str), 1283 (sh, md), 1232 (sh, md), 1202 (sh, str), 1153 (sh, md), 1144 (sh, md), 1116 (sh, str), 1032 (sh, str), 1014 (sh, str). HR-ESI-MS: Calcd for [**L1**+Na]$^+$ ($C_{21}H_{23}N_7O_2Na$) *m/z* 428.1811; Found 428.1772. Elemental analysis calcd for $C_{21}H_{23}N_7O_2 \cdot 0.3H_2O$: C, 61.39; H, 5.79; N, 23.86. Found: C, 61.24; H, 5.74; N, 23.54.

L2. A solution of **4** (0.227 g, 1.48 mmol) and **1** (0.101 g, 0.747 mmol) in EtOH (50 mL) was heated at reflux for 2 h. The white mixture was cooled to RT. The white precipitate was filtered, washed with EtOH and Et_2O then dried under vacuum to give **L2** (0.207 g, 0.503 mmol, 68%) as a white solid. ^{1}H NMR (400 MHz, [D]chloroform) *δ* 7.94 (d, *J* = 7.8 Hz, 2H H-3), 7.80 (s, 2H, H-5), 7.64 (m), 7.52 (s), 7.00 (s), 6.77 (d, *J* = 6.6 Hz, 2H, H-12), 4.70 (d, *J* = 4.70 Hz, 4H, H-15), 3.74 (s, 6H, H-8) ppm. Selected IR *ν*/cm^{-1}: 3316 (br, wk, O-H), 1592 (sh, str), 1572 (sh, str, C=N), 1483 (sh, str), 1458 (sh, str), 1378 (sh, str), 1317 (sh, wk), 1291 (sh, wk), 1250 (sh, md), 1218 (sh, md), 1142 (sh, str), 1082 (sh, wk), 1066 (sh, md), 1028 (sh, md), 1010 (sh, str). HR-ESI-MS: Calcd for [**L2**+Na]$^+$ ($C_{21}H_{23}N_7O_2Na$) *m/z* 428.1805; Found 428.1787. Elemental analysis calcd for $C_{21}H_{23}N_7O_2 \cdot 0.4H_2O$: C, 61.12; H, 5.81; N, 23.76. Found: C, 61.06; H, 5.39; N, 23.48.

L3. A mixture of **2** (0.571 g, 4.16 mmol) and **6** (0.424 g, 1.07 mmol) in EtOH (50 mL) was heated at reflux for 1 h. The yellow mixture was cooled to RT. The yellow precipitate was filtered, washed with EtOH and Et_2O then dried under vacuum to give **L3** (0.359 g, 0.565 mmol, 53%) as a yellow solid. Selected IR *ν*/cm^{-1}: 3164 (br, md, O-H), 1563 (sh, str), 1547 (sh, str, C=N), 1499 (sh, wk), 1476 (sh, md), 1455 (sh, str), 1443 (sh, str), 1398 (sh, str), 1264 (sh, md), 1229 (sh, str), 1133 (sh, str), 1123 (sh, str), 1035 (sh, md), 1007 (sh, md). HR-ESI-MS: Calcd for [**L3**+Na]$^+$ ($C_{37}H_{33}N_9O_2Na$) *m/z* 658.2649; Found 658.2618. Elemental analysis calcd for $C_{37}H_{33}N_9O_2 \cdot 1.5H_2O$: C, 67.05; H, 5.48; N, 19.02. Found: C, 67.64; H, 5.12; N, 18.80.

L4. A solution of **7** (0.253 g, 0.937 mmol) and **6** (0.171 g, 0.430 mmol) in EtOH (50 mL) was heated at 50 °C for 21 h. The brown mixture was cooled to RT. The brown precipitate was filtered, washed with EtOH and Et_2O then dried under vacuum to give **L4** (0.279 g, 0.309 mmol, 72%) as a brown solid. Selected IR *ν*/cm^{-1}: 3253 (br, wk, O-H), 2866 (sh, wk), 1605 (sh, str), 1561 (sh, str), 1547 (sh, str, C=N), 1485 (sh, str), 1440 (sh, str), 1392 (sh, str), 1367 (sh, str), 1308 (sh, md), 1273 (sh, md), 1236 (sh, md), 1216 (sh, md), 1149 (sh, md), 1110 (sh, str), 1004 (sh, str). Elemental analysis calcd for $C_{51}H_{47}N_{15}O_2 \cdot CH_3CH_2OH \cdot 1.5H_2O$: C, 65.28; H, 5.79; N, 21.55. Found: C, 65.33; H, 5.71; N, 21.40.

L5. A solution of **9** (0.475 g, 1.47 mmol) and **6** (0.258 g, 0.649 mmol) in THF (50 mL) was heated at reflux for 22 h. The yellow mixture was cooled to RT. The yellow precipitate was filtered, washed with THF then dried under vacuum to give **L5** (0.399 g, 0.395 mmol, 61%) as a yellow solid. ^{1}H NMR (400 MHz, [D]chloroform) *δ* 8.68 (s), 8.27 (m), 7.96 (dd, *J* = 17.6, 7.8 Hz), 7.88 (d, *J* = 7.3 Hz), 7.85 (m), 7.80 (s), 7.76 (t, *J* = 7.8 Hz), 7.70 (d, *J* = 8.5 Hz), 7.61 (m), 7.52 (s), 7.00 (s), 6.89 (d, *J* = 7.1 Hz), 6.52 (dd, *J* = 17.4, 1.5 Hz, H-38a/b), 6.25 (dd, *J* = 17.3, 10.4 Hz, H-37), 5.91 (dd, *J* = 10.4, 1.4 Hz, H-38a/b), 5.25 (s, H-35), 3.90 (s, H-16/28), 3.72 (s, H-16/28) ppm. Selected IR *ν*/cm^{-1}: 1728 (sh, str, C=O), 1562 (sh, str), 1546 (sh, str, C=N), 1476 (sh, str), 1435 (sh, str), 1397 (sh, str), 1317 (sh, str), 1252 (sh, md), 1215 (sh, md), 1177 (sh, md), 1127 (sh, str), 1065 (sh, md), 1007 (sh, md).

PbL1(CF_3SO_3)$_2$. A mixture of **L1** (0.096 g, 0.26 mmol) and $Pb(CF_3SO_3)_2 \cdot H_2O$ (0.322 g, 0.616 mmol) in CH_3CN (25 mL) was stirred at RT for 5 h and the orange solution evaporated *in vacuo* to an orange solid. The solid was dissolved in CH_3CN (25 mL) and vapour diffused with Et_2O (50 mL) to give Pb**L1**(CF_3SO_3)$_2$ (0.026 g, 0.029 mmol, 12%) as an orange solid. ^{1}H NMR (500 MHz, [D$_4$]methanol): *δ* 8.55 (m, 2H, H-5/11), 8.32 (m, 1H, H-4), 8.00 (m, 2H, H-3/13), 7.51 (d, *J* = 8.7 Hz, H-14), 4.77 (s, 4H, H-15), 3.80 (d, *J* = 0.8 Hz, 3H, H-8) ppm. ^{13}C NMR (126 MHz, [D$_4$]methanol): *δ* 155.4 (C-9), 153.4 (C-2), 145.9 (C-11), 142.7 (C-12), 141.1 (C-13), 137.4 (C-5), 133.3 (C-3), 128.1 (C-4), 111.5 (C-14), 61.9 (C-15), 34.8 (C-8) ppm. Selected IR *ν*/cm^{-1}: 3259 (br, wk, OH), 1598 (sh, md), 1547 (sh, md, C=N), 1496 (sh, md), 1401 (sh, md), 1315 (sh, md), 1238 (br, str, $SO_3CF_3^-$), 1156 (sh, str), 1127 (sh, str), 1023 (sh, str). HR-ESI-MS: Calcd for [**L1**+Pb+CF_3SO_3]$^+$ ($C_{22}H_{23}F_3N_7O_5PbS$) *m/z* 762.1196; Found 762.1233. Elemental analysis calcd for $C_{23}H_{23}F_6N_7O_8PbS_2$: C, 30.33; H, 2.55; N, 10.77. Found: C, 30.37; H, 2.47; N, 10.82. Single crystals of [Pb**L1**(CF_3SO_3)$_2$]$\cdot CHCl_3$ were obtained by vapour diffusion of $CHCl_3$ into a solution of **L1** and two equivalents of $Pb(CF_3SO_3)_2 \cdot H_2O$ in CH_3OH.

PbL2(CF_3SO_3)$_2$. A mixture of **L2** (0.058 g, 0.14 mmol) and $Pb(CF_3SO_3)_2 \cdot H_2O$ (0.112 g, 0.214 mmol) in CH_3CN (25 mL) was stirred at RT for 30 min, filtered, and a 1:1 mixture of PE/Et_2O (150 mL) added to the filtrate to give Pb**L2**(CF_3SO_3)$_2$ (0.082 g, 0.090 mmol, 63%) as a yellow solid. ^{1}H NMR (500 MHz, [D$_4$]methanol): *δ* 8.44 (d, *J* = 1.1 Hz, 2H, H-5), 8.19 (t, *J* = 7.8 Hz, 1H, H-4), 7.90 (dd, *J* = 8.5, 7.5 Hz, 2H, H-13), 7.82 (d, *J* = 7.8 Hz, 2H, H-3), 7.27 (d, *J* = 8.5 Hz, 2H, H-14), 7.07 (dd, *J* = 7.4, 0.9 Hz, 2H, H-12), 4.96 (s, 4H, H-15), 3.74 (d, *J* = 0.9 Hz, 6H, H-8) ppm. ^{13}C NMR (126 MHz, [D$_4$]methanol): *δ* 160.3 (C-11), 156.8 (C-9), 154.2 (C-2), 141.8 (C-13), 141.6 (C-4), 138.8 (C-5), 127.4 (C-3), 116.0 (C-12), 109.4 (C-14), 65.3 (C-15), 34.8 (C-8) ppm. Selected IR *ν*/cm^{-1}: 3335 (sh, br, O-H), 1589 (sh, md), 1548 (sh, md, C=N), 1481 (sh, md), 1433 (sh, md), 1328 (sh, str), 1287 (sh, str), 1221 (br, str, $SO_3CF_3^-$), 1166 (sh, md), 1019 (sh, str). HR-ESI-MS: Calcd for [**L2**+Pb+CF_3SO_3]$^+$ ($C_{22}H_{23}F_3N_7O_5PbS$) *m/z* 762.1196; Found 762.1268. Calcd for [**L2**+Pb-H]$^+$ ($C_{21}H_{22}N_7O_2Pb$) *m/z* 612.1598; Found 612.1651. Elemental analysis calcd for $C_{23}H_{23}F_6N_7O_8PbS_2$: C, 30.33; H, 2.55; N, 10.77. Found: C, 30.38; H, 2.42; N, 10.70. Single crystals of Pb**L2**(CF_3SO_3)$_2$][Pb**L2**CF_3SO_3]$CF_3SO_3 \cdot CH_3CN$ were obtained by vapour diffusion of Et_2O into a solution of **L2** and one equivalent of $Pb(CF_3SO_3)_2 \cdot H_2O$ in CH_3CN.

Pb_2L3(CF_3SO_3)$_4$. A mixture of **L3** (0.025 g, 0.039 mmol) and $Pb(CF_3SO_3)_2 \cdot H_2O$ (0.085 g, 0.16 mmol) in CH_3CN (25 mL) was stirred at RT for 1 h and the yellow solution evaporated *in vacuo* to a yellow solid. The solid was dissolved in CH_3CN (5 mL) and vapour diffused with Et_2O to give Pb_2**L3**(CF_3SO_3)$_4$ (0.026 g, 0.016 mmol, 41%) as a yellow solid. ^{1}H NMR (500 MHz, [D$_3$]acetonitrile): *δ* 8.52 (s, 1H, H-18), 8.45 (s, 1H, H-3), 8.24 (dd, *J* = 8.6, 7.5 Hz, 1H, H-9), 8.06 (t, *J* = 7.8 Hz, 1H, H-23), 8.02 (m, 1H, H-12/13/14), 7.96 (d, *J* = 7.5 Hz, 1H, H-10), 7.74 (dd, *J* = 7.7, 1.1 Hz, 1H, H-24), 7.63 (m, 2H, H-12/13/14), 7.55 (d, *J* = 8.7 Hz, 1H, H-8), 7.47 (d, *J* = 7.9 Hz, 1H, H-22), 4.91 (d, *J* = 4.5 Hz, 2H, H-25), 4.87 (m, 1H, H-26), 3.71 (d, *J* = 0.8 Hz, 4H, H-16) ppm. ^{13}C NMR (126 MHz, [D$_3$]acetonitrile): *δ* 161.9 (C-21), 157.5 (C-2), 156.6 (C-7), 155.0 (C-5), 154.3 (C-11), 151.3 (C-19), 143.3 (C-9), 141.5 (C-23), 141.0 (C-18), 137.5 (C-4), 131.5 (C-14), 130.5 (C-12/13), 128.7 (C-12/13), 126.6 (C-24), 124.7 (C-3), 124.0 (C-22), 120.2 (C-10), 118.3 (C-8), 65.1 (C-25), 36.5 (C-16) ppm. Selected IR *ν*/cm^{-1}: 3420 (br, wk, O-H), 1595 (sh, md), 1574 (sh, md, C=N), 1562 (sh, md), 1483 (sh, md), 1460 (sh, md), 1209 (br, str, $SO_3CF_3^-$), 1165 (sh, str), 1015 (sh, str). HR-ESI-MS: Calcd for [**L3**+Pb_2+CF_3SO_3-H]$^{2+}$ ($C_{38}H_{32}F_3N_9O_5Pb_2S$) *m/z* 599.5864; Found 599.5812. Calcd for [**L3**+Pb]$^{2+}$ ($C_{37}H_{33}N_9O_2Pb$) *m/z* 421.6259; Found 421.6228. Calcd for [**L3**+Pb_2-2H]$^{2+}$ ($C_{37}H_{31}N_9O_2Pb_2$) 524.6066; Found 524.6024. Calc for [**L3**+Pb_2+Br-H]$^{2+}$ ($C_{37}H_{32}BrN_9O_2Pb_2$) 564.5686; Found 564.5643. Elemental analysis calcd for $C_{41}H_{33}F_{12}N_9O_{14}Pb_2S_4$: C, 29.91; H, 2.02; N, 7.66. Found: C, 30.11; H, 2.14; N, 7.40. Single crystals of [Pb_2**L3**(CF_3SO_3)$_2$Br]$CF_3SO_3 \cdot CH_3CN$ were

Accepted Manuscript

This article is protected by copyright. All rights reserved.

obtained by vapour diffusion of Et_2O into a solution of **L3** and four equivalents of $Pb(CF_3SO_3)_2{\cdot}H_2O$ in CH_3CN.

$Pb_2L4(CF_3SO_3)_4$. A mixture of **L4** (0.059 g, 0.065 mmol) and $Pb(CF_3SO_3)_2{\cdot}H_2O$ (0.152 g, 0.290 mmol) in CH_3CN (25 mL) was stirred at RT for 30 min and the orange solution evaporated *in vacuo* to a yellow oil. The oil was dissolved in CH_3CN (2 mL) and vapour diffused with Et_2O (20 mL) to give Pb_2**L4**$(CF_3SO_3)_4$ (0.061 g, 0.032 mmol, 49%) as an orange solid. ^{1}H NMR (400 MHz, [D$_3$]acetonitrile): δ 8.36 (t, J = 7.7 Hz, 1H, H-23), 8.32 (s, 1H, H-3), 8.19 (s, 1H, H-18), 8.11 (t, J = 8.0 Hz, 1H, H-33), 8.01 (dd, J = 6.6, 3.0 Hz, 1H, H-10), 7.93 (d, J = 7.7 Hz, 1H, H-24), 7.69 (m, 4H, H-9/12/13/14), 7.59 (d, J = 7.7 Hz, 1H, H-22), 7.50 (m, 2H, H-25/34), 7.04 (d, J = 8.8 Hz, 1H, H-8), 6.84 (s, 1H, H-31), 3.87 (d, J = 10.4 Hz, 2H, H-35), 3.41 (s, 3H, H-28), 3.27 (s, 3H, H-16) ppm. Selected IR ν/cm^{-1}: 3413 (br, wk, O-H), 3085 (br, wk), 1590 (sh, md), 1571 (sh, md), 1542 (sh, md, C=N), 1492 (sh, md), 1396 (sh, md), 1315 (sh, md), 1279 (sh, str), 1221 (br, str, $SO_3CF_3^-$), 1150 (sh, str), 1125 (sh, str), 1050 (sh, md), 1020 (sh, str). HR-ESI-MS: Calcd for [**L4**+Pb]$^{2+}$ ($C_{51}H_{47}N_{15}O_2Pb$) m/z 554.6899; Found 554.6867. Elemental analysis calcd for $C_{55}H_{47}F_{12}N_{15}O_{14}Pb_2S_4$: C, 34.54; H, 2.48; N, 10.98. Found: C, 34.63; H, 2.57; N, 11.12. Single crystals of [Pb_2**L4**$(CF_3SO_3)_3]CF_3SO_3{\cdot}CH_3CN$ were obtained by vapour diffusion of Et_2O into a solution of **L4** and five equivalents of $Pb(CF_3SO_3)_2{\cdot}H_2O$ in CH_3CN. Single crystals of [Pb_2**L4**$CF_3SO_3(CH_3OH)_2](CF_3SO_3)_3{\cdot}2CH_3OH{\cdot}2H_2O$ were obtained by vapour diffusion of Et_2O into a solution of **L4** and five equivalents of $Pb(CF_3SO_3)_2{\cdot}H_2O$ in CH_3OH.

Reaction of L5 with $Pb(CF_3SO_3)_2{\cdot}H_2O$. A mixture of **L5** (0.020 g, 0.020 mmol) and $Pb(CF_3SO_3)_2{\cdot}H_2O$ (0.052 g, 0.099 mmol) in CH_3CN (25 mL) was stirred at RT for 2 h and the orange solution evaporated *in vacuo* to a yellow solid. The solid was dissolved in CH_3CN (2 mL) and vapour diffused with Et_2O (20 mL) to give an orange solid (0.046 g). Selected IR ν/cm^{-1}: 1718 (sh, md, C=O), 1594 (sh, md), 1574 (sh, md), 1546 (sh, md, C=N), 1482 (sh, md), 1454 (sh, md), 1407 (sh, md), 1206 (br, str, $SO_3CF_3^-$), 1162 (sh, str), 1012 (sh, str). HR-ESI-MS: Calcd for [**L5**+Pb+CF_3SO_3]$^+$ ($C_{58}H_{51}F_3N_{15}O_7PbS$) m/z 1366.3536; Found 1366.3523. Calcd for [**L5**+Pb]$^{2+}$ ($C_{57}H_{51}N_{15}O_4Pb$) m/z 608.7006; Found 608.7083. Single crystals of [Pb_3**L5**$(CF_3SO_3)_5]CF_3SO_3{\cdot}3CH_3CN{\cdot}Et_2O$ were obtained by vapour diffusion of Et_2O into a solution of the bulk solid in CD_3CN.

Keywords: single helicate • lead • supramolecular chemistry

[1] A. M. Stadler, J. Ramírez, J. M. Lehn, *Chem. Eur. J.* **2010**, *16*, 5369-5378.

[2] M. Barboiu, A. M. Stadler, J. M. Lehn, *Angew. Chem. Int. Ed.* **2016**, *55*, 4130-4154.

[3] a) M. Stadler, N. Kyritsakas, G. Vaughan, J. M. Lehn, *Chem. Eur. J.* **2007**, *13*, 59-68; b) Barboiu, J. M. Lehn, *Proc. Natl. Acad. Sci. U. S. A.* **2002**, *99*, 5201-5206.

[4] a) D. Curry, M. A. Robinson, D. H. Busch, *Inorg. Chem.* **1967**, *6*, 1570-1574; b) Wester, G. J. Palenik, *Inorg. Chem.* **1976**, *15*, 755-761.

[5] a) J. Horn, A. J. Blake, N. R. Champness, A. Garau, V. Lippolis, C. Wilson, M. Schroder, *Chem. Commun.* **2003**, 312-313; b) J. Horn, A. J. Blake, N. R. Champness, V. Lippolis, M. Schroder, *Chem. Commun.* **2003**, 1488-1489; c) J. Wang, Y. C. Wang, H. C. Kao, *J. Chin. Chem. Soc.* **2010**, *57*, 876-882; d) Kennepohl, A. Thomas, R. McDonald, *Acta Crystallogr., Sect. E.* **2006**, *62*, 2967-2969.

[6] C. Piguet, G. Bernardinelli, G. Hopfgartner, *Chem. Rev.* **1997**, *97*, 2005-2062.

[7] a) Barboiu, G. Vaughan, R. Graff, J. M. Lehn, *J. Am. Chem. Soc.* **2003**, *125*, 10257-10265; b) M. Senegas, S. Koeller, G. Bernardinelli, C. Piguet, *Chem. Commun.* **2005**, 2235-2237; c) K. Al-Rasbi, H. Adams, L. P. Harding, M. D. Ward, *Eur. J. Inorg. Chem.* **2007**, *2007*, 4770-4780; d) Eerdun, S. Hisanaga, J. Setsune, *Chem. Eur. J.* **2015**, *21*, 239-246; e) S. Tsang, C. C. Yee, S. M. Yiu, W. T. Wong, H. L. Kwong, *Polyhedron.* **2014**, *83*, 167-177; f) Liu, H. Zhou, Z. Q. Pan, D. Hu, Q. M. Huang, H. P. Zhang, X. L. Hu, X. G. Meng, *Inorg. Chem. Commun.* **2007**, *10*, 805-807.

[8] a) P. Thummel, C. Hery, D. Williamson, F. Lefoulon, *J. Am. Chem. Soc.* **1988**, *110*, 7894-7896; b) J. Cathey, E. C. Constable, M. J. Hannon, D. A. Tohcer, M. D. Ward, *J. Chem. Soc., Chem. Commun.* **1990**, 621-622; c) L. Kwong, H. L. Yeung, W. S. Lee, W. T. Wong, *Chem. Commun.* **2006**, 4841-4843.

[9] P. K. K. Ho, K. K. Cheung, S. M. Peng, C. M. Che, *J. Chem. Soc., Dalton Trans.* **1996**, 1411-1417.

[10] A. M. Stadler, N. Kyritsakas, J. M. Lehn, *Chem. Commun.* **2004**, 2024-2025.

[11] a) M. Najar, I. S. Tidmarsh, M. D. Ward, *CrystEngComm.* **2010**, *12*, 3642-3650; b) J. Romero, R. Carballido, L. Rodriguez-Silva, M. Maneiro, G. Zaragoza, A. M. Gonzalez-Noya, R. Pedrido, *Dalton Trans.* **2016**, *45*, 16162-16165.

[12] D. J. Hutchinson, L. R. Hanton, S. C. Moratti, *Inorg. Chem.* **2011**, *50*, 7637-7649.

[13] A. M. Stadler, J. M. Lehn, *J. Am. Chem. Soc.* **2014**, *136*, 3400-3409.

[14] a) C. Kao, Y. C. Wang, W. J. Wang, *Res. Chem. Intermed.* **2017**, *43*, 3539-3552; b) J. Fu, W. Y. Sun, W. N. Dai, M. H. Shu, F. Xue, D. F. Wang, T. C. W. Mak, W. X. Tang, H. W. Hu, *Inorg. Chim. Acta.* **1999**, *290*, 127-132; c) Onodera, G. Hirata, T. Seike, R. Takeuchi, M. Kimura, *Polyhedron.* **2016**, *112*, 43-50.

[15] H. E. Gottlieb, V. Kotlyar, A. Nudelman, *J. Org. Chem.* **1997**, *62*, 7512-7515.

[16] Agilent, Agilent Technologies Ltd, Yarnton, Oxfordshire, England, **2014**.

[17] Z. Otwinowski, W. Minor, *Methods Enzymol.* **1997**, *276*, 307-326.

[18] G. M. Sheldrick, University of Göttingen, Göttingen, **1996**.

[19] G. M. Sheldrick, *Acta Crystallogr., Sect. A.* **2015**, *71*, 3-8.

[20] A. Altomare, M. C. Burla, M. Camalli, G. L. Cascarano, C. Giacovazzo, A. Guagliardi, A. G. G. Moliterni, G. Polidori, R. Spagna, *J. Appl. Crystallogr.* **1999**, *32*, 115-119.

[21] G. M. Sheldrick, *Acta Crystallogr., Sect. C.* **2015**, *71*, 3-8.

[22] L. Farrugia, *J. Appl. Crystallogr.* **2012**, *45*, 849-854.

[23] A. Spek, *Acta Crystallogr., Sect. D.* **2009**, *65*, 148-155.

[24] C. F. Macrae, I. J. Bruno, J. A. Chisholm, P. R. Edgington, P. McCabe, E. Pidcock, L. Rodriguez-Monge, R. Taylor, J. van de Streek, P. A. Wood, *J. Appl. Crystallogr.* **2008**, *41*, 466-470.

[25] N. T. Coogan, M. A. Chimes, J. Raftery, P. Mocilac, M. A. Denecke, *J. Org. Chem.* **2015**, *80*, 8684-8693.

[26] N. M. Shavaleev, R. Scopelliti, F. Gumy, J. C. G. Bünzli, *Inorg. Chem.* **2009**, *48*, 6178-6191.

[27] F. S. Han, M. Higuchi, D. G. Kurth, *Org. Lett.* **2007**, *9*, 559-562.

Accepted Manuscript

This article is protected by copyright. All rights reserved.

10.1002/asia.201801784

Entry for the Table of Contents (Please choose one layout)

Layout 1:

FULL PAPER

Single-mindedly. The multidentate pyridine-hydrazone ligands self-assemble with Pb^{II} into single-stranded helicates. Other supramolecular structures such as single-stranded *meso*-helicates and double-stranded helicates are not favoured because of the low coordinative saturation of Pb^{II} by the ligands.

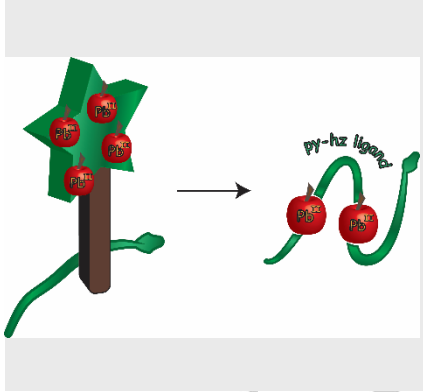

*Maureen J. Lobo, Stephen C. Moratti, and Lyall R. Hanton**

Page No. – Page No.

A Design Strategy for Single-Stranded Helicates using Pyridine-Hydrazone Ligands and Pb^{II}

Layout 2:

FULL PAPER

((Insert TOC Graphic here; max. width: 11.5 cm; max. height: 2.5 cm))

*Author(s), Corresponding Author(s)**

Page No. – Page No.

Title

Text for Table of Contents

Accepted Manuscript

This article is protected by copyright. All rights reserved.